Macromolecular Bioscience
www.mbs-journal.de

Carbon Nanotube Reinforced Supramolecular Hydrogels for Bioapplications

*Marko Mihajlovic, Milos Mihajlovic, Patricia Y. W. Dankers, Rosalinde Masereeuw, and Rint P. Sijbesma**

Nanocomposite hydrogels based on carbon nanotubes (CNTs) are known to possess remarkable stiffness, electrical, and thermal conductivity. However, they often make use of CNTs as fillers in covalently cross-linked hydrogel networks or involve direct cross-linking between CNTs and polymer chains, limiting processability properties. Herein, nanocomposite hydrogels are developed, in which CNTs are fillers in a physically cross-linked hydrogel. Supramolecular nanocomposites are prepared at various CNT concentrations, ranging from 0.5 to 6 wt%. Incorporation of 3 wt% of CNTs leads to an increase of the material's toughness by over 80%, and it enhances electrical conductivity by 358%, compared to CNT-free hydrogel. Meanwhile, the nanocomposite hydrogels maintain thixotropy and processability, typical of the parent hydrogel. The study also demonstrates that these materials display remarkable cytocompatibility and support cell growth and proliferation, while preserving their functional activities. These supramolecular nanocomposite hydrogels are therefore promising candidates for biomedical applications, in which both toughness and electrical conductivity are important parameters.

1. Introduction

Hydrogels are materials composed of hydrophilic polymers crosslinked into a 3D network.[1] They represent a very attractive class of materials due to their soft nature and ability to absorb water. Hydrogels mimic biological environments and, as such, they are promising materials for constructing scaffolds for biomedical applications.[2–5] To this end, it is required to develop hydrogels that are both biocompatible and mechanically tough.

There is a large demand for hydrogels which are easy to prepare, and which have multiple functionalities, and tunable properties. In the past decades, a new class of hydrogels, known as nanocomposite hydrogels,[6] has been designed to improve mechanical performance. These gels, next to the polymeric network, contain inorganic particles, such as clay, graphene, carbon nanotubes (CNTs), or silica.[7] Besides improving mechanical properties, new optical, electrical, and thermal properties are imparted to the nanocomposite material due to the inorganic component.[8–10]

CNTs are widely used to make nanocomposite hydrogels because of their unique properties, such as electrical and thermal conductivity, high mechanical strength, high specific area, and low mass density.[11] CNTs are often used as reinforcing agents to enhance the mechanical properties of hydrogels. By incorporating CNTs in hydrogel formulations, it is possible to obtain very tough[12,13] and electrically conductive hydrogels.[14–17] CNT-based nanocomposites represent a versatile platform for developing hydrogels with multiple responsive properties and remarkable mechanical performance. However, there is a concern about the toxic effects of CNTs and, therefore, hydrogel biocompatibility. Studies reported CNT toxicity that seemed to be dose-dependent, but which could be reduced when CNTs are functionalized and incorporated in networks.[15,18]

Most of the reported CNT-based nanocomposite hydrogels contain covalent cross-links between CNTs and polymer chains, or between polymer chains, with CNTs being only physically embedded in the network.[13,14,19–22] In addition, some of the preparation procedures are quite complicated and laborious due to the challenges in dispersing CNTs efficiently in the matrix. In addition to improved mechanical behaviour, various responsive properties, and biocompatibility, it would be an asset to have completely physically crosslinked networks, which in contrast to covalent systems,

M. Mihajlovic, Prof. R. P. Sijbesma
Laboratory of Macromolecular and Organic Chemistry
Department of Chemical Engineering and Chemistry
Eindhoven University of Technology
P.O. Box 513, 5600 MB Eindhoven, The Netherlands
E-mail: r.p.sijbesma@tue.nl
M. Mihajlovic, Prof. P. Y. W. Dankers, Prof. R. P. Sijbesma
Institute for Complex Molecular Systems
Eindhoven University of Technology
P.O. Box 513, 5600 MB Eindhoven, The Netherlands
M. Mihajlovic, Prof. R. Masereeuw
Division of Pharmacology
Utrecht Institute for Pharmaceutical Sciences
Utrecht University
3584 CG Utrecht, The Netherlands
Prof. P. Y. W. Dankers
Department of Biomedical Engineering
Laboratory of Chemical Biology
Eindhoven University of Technology
P.O. Box 513, 5600 MB Eindhoven, The Netherlands
The ORCID identification number(s) for the author(s) of this article can be found under https://doi.org/10.1002/mabi.201800173.

DOI: 10.1002/mabi.201800173

would allow for easy processability, manipulation, and reshaping features of the hydrogels. To the best of our knowledge, there are limited studies on physical nanocomposite gels containing CNTs. Some of the described systems are based on PVA[23] or alginate.[24] However, these gels are either not tested for biocompatibility or lack significant improvement in physical or mechanical properties of the polymer counterpart, with processability not being discussed.

In the present work, these properties were targeted in a single, fully physically cross-linked nanocomposite hydrogel, whose fabrication is simple and easy. The aim was to develop a CNT-based hydrogel that is characterized by high toughness, electrical conductivity, processability, and biocompatibility, as all of these features are essential for bioapplications. We chose to work with a hydrophobically associating physical hydrogel, which we developed previously.[25] The polymer forming the gel is a segmented copolyester of polyethylene glycol (PEG, Mw 2000) and dimer fatty acid (DFA). The segmented copolymer gives rise to a stable and free-standing hydrogel due to strong hydrophobic associations between DFA segments. It was estimated that each DFA nanodomain is composed of approximately 200 DFA units. It was shown that this hydrogel is processable and displays high toughness, therefore it was combined with CNTs in order to improve the toughness and to achieve new functionalities and properties. In particular, short multi-walled CNTs (MWNTs) were employed, so as to achieve easier functionalization and dispersion in the hydrogel. We anticipated that this PEG/DFA/MWNT nanocomposite hydrogel would result in a material with tunable physical, mechanical, and biochemical properties.

Herein, the development and easy fabrication of purely physically assembled nanocomposite hydrogels, at different MWNT content and without covalent cross-links, is described. In addition, detailed physical and mechanical characterization, hydrogel's biocompatibility and interaction with conditionally immortalized renal proximal tubule epithelial cells (ciPTEC) and cervical adenocarcinoma epithelial cells (HeLa) were addressed.

2. Experimental Section

2.1. Materials

Multi-walled nanotubes (MWNT) were purchased from Nanoamor Inc. (stock# 1237YJS, 95%, OD 20–30 nm, length 0.5-2 μm). The segmented copolymer PE PEG2000 was synthesized as described previously,[25] yielding the polymer with M_n of 42 kg mol^{-1} and PDI of 2.07. Poly(ethylene glycol) 2000 (PEG 2000) was purchased from Merck. Tin (II) chloride anhydrous ($SnCl_2$) (99%) was obtained from Alfa Aesar. Dimer fatty acid (DFA) was purchased from Sigma-Aldrich. Concentrated sulfuric acid (H_2SO_4, 98%), nitric acid, (HNO_3, 65%), and bulk solvents were obtained from Biosolve BV Chemicals. PEG was dried by azeotropic distillation with toluene before use, all other reagents were used without further purification.

2.2. Oxidation of MWNT

Oxidized MWNT (ox-MWNT) were prepared according to the reported procedure.[26] Briefly, 350 mg of pristine MWNT were dispersed in the mixture of sulfuric and nitric acid (3:1, v/v) and sonicated for 24 h at room temperature (RT). Deionized water was then slowly added (at 0 °C) to dilute the mixture and ox-MWNT were filtered (Millipore, JHWP 0.45 μm filter), resuspended in water and washed until the pH of the filtrate was neutral. The black powder was dried under vacuum overnight to yield 304 mg of ox-MWNT.

2.3. Fabrication of Nanocomposite Hydrogel

PE PEG2000 was synthesized by a polycondensation reaction in the melt, under vacuum, between PEG2000 and DFA. Segmented copolymer and oxidized MWNT were used to prepare the nanocomposite hydrogels at four different CNT contents (0.5, 1.5, 3, and 6 wt% relative to the weight of PE PEG2000). In order to embed ox-MWNT homogeneously within the polymer network, we made use of the following procedure: typically, 0.5 wt% MWNT sample was prepared by dispersing 1.5 mg of ox-MWNTs in 0.8 mL water and sonication at RT for 2 h. PE PEG2000 copolymer (300 mg) was dissolved in 2 mL of acetone. Next, the aqueous solution of ox-MWNT was added to the acetone solution of PE PEG2000 and the resulting blend was mixed thoroughly. Additional 0.5 mL of water was added, until a semisolid gel was formed. At this point, ox-MWNT were completely absent from the liquid and incorporated in the gel phase. After blending, the gel was kept in a large amount of deionized water for a day, with water changed several times in order to remove the remaining acetone. The hydrogel was then dried in an oven, under reduced pressure, at 40 °C for 24 h. The obtained dry material was then used for making homogeneous samples by compression molding. The material was press-melted at 95 °C and at 100 bar for 10 min, using a stainless steel mold. Teflon sheets were used to prevent the material from sticking. After cooling down to ambient temperature, polymer nanocomposite disks were removed from the mold, weighed, and placed in water for at least 24 h to yield 0.5 wt% MWNT nanocomposite hydrogel. The prepared polymer disks were 0.5 mm thick, with 25 mm diameter. Following the same procedure, hydrogels at 1.5, 3, and 6 wt% MWNT content were prepared, using the appropriate amount of ox-MWNT and adjusting the volume of water. The control sample was fabricated in the same way, with the exception that pure water instead of CNT solution was used.

2.4. Equilibrium Water Content and Stability of Hydrogels

Equilibrium water contents (EWCs) of the hydrogels was determined by the gravimetric method. Dry polymer disks were weighed and placed in a large amount of water for at least 24 h until they reached the equilibrium swelling state. The amount of water absorbed by materials was determined by taking the disks from the water bath and gently blotting with paper to remove the surface water. Then, the weight was recorded and the amount of water determined with the following equation:

$$\mathrm{EWC}(\%) = \frac{m - m_d}{m} \cdot 100 \quad (1)$$

where m_d and m are the weights of the dry sample and hydrogel at the moment of measurement, respectively.

The stability of the nanocomposite hydrogels at swelling equilibrium was investigated by the same method. The stability was tested in different conditions. In the first case, hydrogels were stirred in deionized water at RT and the weights were recorded at defined times for the next 20 days. Fresh water was replaced each time the measurement took place. Additionally, their stability was assessed in physiological conditions. Hydrogels were swollen and then stirred in large volume of PBS, at 37 °C, and the weight was monitored over a period of 20 days.

2.5. Thermogravimetric Analysis

The measurements were performed on a thermogravimetric analysis (TGA) Q500 instrument using the following procedure: 1 mg of either pristine MWNT or ox-MWNT was subjected to an isotherm at 100 °C for 20 min, then it was heated from 100 to 700 °C at a heating rate of 10 °C min^{-1} and under the N_2 flow (90 mL min^{-1}). Data were analyzed with the TA Universal Analysis 2000 software.

2.6. Transmission Electron Microscopy

Transmission electron microscopy (TEM) analysis of CNTs was performed on a Tecnai Sphera electron microscope (FEI Company), equipped with an LaB_6 filament that was operated at an accelerating voltage of 200 kV. Images were acquired using a bottom mounted 1024 × 1024 Charge-coupled device (CCD) camera. Samples were prepared by dispersing nanotubes in DMF at a concentration of 0.1 mg mL^{-1}. After sonicating the dispersion for 1 h, one drop was deposited on a carbon-coated copper grid (CF300-Cu, Electron Microscopy Sciences) and dried in a vacuum oven at 40 °C overnight.

2.7. Scanning Electron Microscopy

Morphology of nanocomposite hydrogels was studied by scanning electron microscopy (SEM; FEI Quanta 3D FEG), at an accelerating voltage of 5.00 kV. Equilibrium-swollen hydrogels were frozen in liquid nitrogen, immediately cut with a sharp scalpel to expose the cross section, and then freeze-dried for 48 h. Prior to imaging, samples were sputtered with a thin layer of gold for 120 s.

2.8. Conductivity Measurements

Hydrogel samples were prepared by swelling and keeping nanocomposite polymer films in Milli-Q purified water for 14 days, with water changed at least ten times, to remove ions and impurities derived from the fabrication and preparation process. Resistivity of the hydrogels was assessed via the four-point method with parallel electrodes, separated by 5 mm. Current at different intensities was applied through the external electrodes by a Keithley 237 source, and the voltage between the inner electrodes was recorded by a Keithely 6517A electrometer. Data were plotted in a V–I graph, and the resistance was calculated as the slope of the linear response (Ohmic region). Conductivity σ, expressed in S m^{-1}, was calculated by using the following equation:

$$\sigma = \frac{d}{R \cdot H \cdot W} \tag{2}$$

where d is the distance between the electrodes (5 mm), R is the resistance obtained from the V–I plot, H is the sample thickness (0.85 mm), and W is the sample width (15.5 mm). Conductivity was determined on three samples and the value was averaged.

2.9. Rheology

Viscoelastic properties of the PE PEG2000 and nanocomposite hydrogel were measured by a stress-controlled rheometer (Anton Paar, Physica MCR501), equipped with a 25 mm plate geometry and a Peltier chamber, to control the temperature and protect the samples from drying. All measurements were conducted on hydrogel samples at swelling equilibrium, either at 25 °C or 37 °C, as will be specified further in the text. For measurements at 37 °C the hydrogels were swollen with PBS solution. Frequency sweep measurements were performed over a frequency range of 0.1–100 rad s^{-1}, at 0.1% strain, both at 25 °C and 37 °C. During the dynamic amplitude test the frequency was kept constant at 1 rad s^{-1}, the strain was alternated between 0.1 and 200% and the duration of one cycle was set at 200 s.

2.10. Tensile Testing

The tensile mechanical properties of the hydrogels were measured using a Zwick Z100 Universal Tensile Tester machine, equipped with the load cell of 100 N. All measurements were done at RT and at the crosshead speed of 10 mm min^{-1}. Equilibrium-swollen hydrogel disks were cut in dog-bone shaped samples, whose size was 12.5 mm length, 2 mm width, and 0.85 mm thickness. Each sample was tightly fixed between the clamps, with the overall gage length of 20 mm. The measurements were performed on at least three samples for each hydrogel composition and the results were averaged. From the stress–strain curve, tensile modulus was determined as the slope of the linear response (4–10%), by linear regression method. The tensile strength corresponds to the maximum stress experienced by the material before breaking, whereas the elongation at break was defined as displacement λ (ratio between the sample length at break and its original length). Tensile toughness was calculated by integrating the area under the curve.

2.11. Cell Culture

Urine-derived and organic anion transporter 1 (OAT1) protein overexpressing conditionally immortalized proximal tubule epithelial cells (ciPTEC-OAT1) were cultured in Dulbecco's Modified

Eagle Medium/Nutrient Mixture F-12 (1:1 DMEM/F-12) (Gibco, Life Technologies, Paisly, UK) supplemented with 10% v/v fetal calf serum (FCS) (Greiner Bio-One, Alphen aan den Rijn, the Netherlands), 5 μg mL^{-1} insulin, 5 μg mL^{-1} transferrin, 5 μg mL^{-1} selenium, 35 ng mL^{-1} hydrocortisone, 10 ng mL^{-1} epidermal growth factor, and 40 pg mL^{-1} tri-iodothyronine (all from Sigma-Aldrich, Zwijndrecht, the Netherlands), creating a complete cell culture medium, as reported previously.[27] CiPTEC-OAT1 were cultured up to 60 passages. Since the cells were conditionally immortalized with a temperature-sensitive SV40 large T antigen,[28] cells were cultured at 33 °C and 5% v/v CO_2 to allow proliferation, while the differentiation and maturation was achieved after 7 days of incubation at 37 °C, 5% v/v CO_2, changing the medium every second day.

2.12. Preparation of Gel Extracts

In order to test the effects of hydrogel extracts on cell viability, elution test method was performed according to ISO 10993–5 protocols for cytotoxicity of biomedical devices.[29] Extracts were obtained by incubating all hydrogel samples separately in complete cell culture medium for either 1 or 7 days at 37 °C, 5% v/v CO_2, respecting the ratio of surface area of the gel to the volume of the medium equal to 3 cm^2 mL^{-1}. Latex was used as a negative control. The obtained culture medium was applied on cell monolayers for a period of 24 h and 48 h, during and after which cells were monitored for morphological changes and viability.

2.13. Cell Viability Assay

Cells were seeded on 96-well plates (Costar 3599; Corning, NY, USA) at a density of 55 000 cell cm^{-2}, allowed to adhere and proliferate for 24 h at 33 °C, 5% v/v CO_2, and incubated at 37 °C, 5% v/v CO_2 for 7 days to allow maturation. Afterward, the cells were co-incubated either with PE PEG2000 control and CNT containing hydrogel samples (disks of 1.5 mm diameter and 0.85 mm thickness) or with gel extracts (obtained as already mentioned) for 24 and 48 h, at 37 °C, 5% v/v CO_2. Following the incubation period, cell viability was determined using PrestoBlue cell viability reagent (LifeTechnologies, Paisly, UK) as suggested by the manufacturer. Briefly, 100 μL of the PrestoBlue reagent (1:10 in complete cell culture medium) was added to each well and the cells were incubated for additional 1 h at 37 °C, 5% v/v CO_2 in the dark. Finally, the fluorescence was measured using a fluorescent microplate reader (Fluoroskan Ascent FL, Thermo Fisher Scientific, Vantaa, Finland), at excitation wavelength of 530 nm and emission wavelength of 590 nm. The obtained fluorescence values were corrected for the background, normalized to the untreated cells control and plotted as relative cell viability.

2.14. CiPTEC-OAT1 Culture on Hydrogels

For cell culture, round-shaped pieces of the hydrogels (diameter 6 mm, thickness 0.85 mm, approximate surface growth area 0.28 cm^2) were cut out from compressed molded samples, sterilized with 0.2% v/v solution of peracetic acid (Sigma-Aldrich, Zwijndrecht, the Netherlands) in 4% v/v ethanol for 45 min, and then extensively rinsed three times with HBSS and left in HBSS for additional 24 h. Afterward, small disks of hydrogels were introduced in empty wells of 96-well plates and the L-DOPA (L-3,4-dihydroxyphenylalanine, Sigma-Aldrich, Zwijndrecht, the Netherlands) coating was applied on the gels to support cell attachment and growth, based on previously published studies.[30,31] L-DOPA was dissolved in 10 mM Tris buffer (pH 8.5) at 37 °C for 45 min with occasional mixing, filter sterilized, and applied on hydrogel surface at 2 mg mL^{-1} final concentration for 5 h at 37 °C, as described previously.[32] Following the coating procedure, hydrogels were washed in HBSS and used further for cell seeding.

2.15. Cell Proliferation on Hydrogels

For cell proliferation assay, a total of 18 000 cells per hydrogel sample (surface growth area 0.28 cm^2) were seeded and incubated at 33 °C, 5% v/v CO_2. PrestoBlue cell viability reagent was applied after 1, 4, and 7 days to determine cell proliferation, as described previously for the cell viability assay. Measured fluorescence values for each sample, proportional to the number of viable cells, were corrected for the background and presented as relative a.u. of fluorescence.

2.16. CiPTEC-OAT1 Visualization on Hydrogels

In order to visualize ciPTEC-OAT1 cells on different hydrogel samples, cells were seeded at a density of 45 000 cells per hydrogel (surface growth area 0.28 cm^2), on 96-well plates, and incubated at 33 °C, 5% v/v CO_2 for 24 h followed by 7 days incubation at 37 °C, 5% v/v CO_2, as mentioned previously. After 7 days incubation cell were stained for actin filaments using Phalloidin-FITC (Sigma-Aldrich, Zwijndrecht, the Netherlands) to visualize cell distribution and morphology. Briefly, cells were washed with HBSS three times, fixed with 2% w/v paraformaldehyde in PBS containing 4% w/v sucrose (Sigma-Aldrich, Zwijndrecht, the Netherlands) for 10 min, then washed three times with 0.1% v/v Tween (Sigma-Aldrich, Zwijndrecht, the Netherlands) solution in PBS and permeabilized with 0.3% v/v Triton (Merck, Darmstadt, Germany) solution for 15 min. After another three washing steps with 0.1% v/v Tween-PBS, cells were incubated with phalloidin-FITC (1:250 in PBS) for 1 h at RT and in the dark. Finally, hydrogel disks were mounted on the Willco glass bottom dishes (WillCo Wells B.V., Amsterdam, The Netherlands), using ProLong Gold antifade reagent containing DAPI (Life Technologies, Eugene, OR, USA), and cells were imaged using confocal microscope (Leica TCS SP8 X, Leica Microsystems CMS GmbH, Wetzlar, Germany). Analysis was performed using Leica Application Suite X software (Leica Microsystems CMS GmbH).

2.17. Live/Dead Viability Assay

CiPTEC-OAT1 cells were seeded on hydrogel disks on 96-well plates at a density of 45 000 cells per hydrogel (surface growth

area 0.28 cm^2) and incubated at 33 °C, 5% v/v CO_2 for 24 h. Following 7 days maturation at 37 °C, 5% v/v CO_2, cells were washed twice with warm HBSS and incubated with calcein-AM (2 μM; Life Technologies, Eugene, OR, USA) and ethidium homodimer-1 (EthD-1; 2 μM; Life Technologies, Eugene, OR, USA) diluted in HBSS, for 1 h at 37 °C in the dark. Next, cells were washed once with HBSS and hydrogel samples were mounted on the Willco glass bottom dishes using Dako Fluorescence mounting medium (DAKO, Carpinteria, CA, USA). Visualization was performed using confocal microscope (Leica TCS SP8 X) and analysis using Leica Application Suite X software.

2.18. Fluorescein Assay for OAT1 Activity Measurement

The fluorescein uptake assay was used to determine the OAT1 activity of ciPTEC-OAT1 cultured on hydrogels. In brief, cells were seeded on hydrogel disks with surface growth area of 0.28 cm^2 (45 000 cells per hydrogel sample) on 96-well plates and incubated at 33 °C, 5% v/v CO_2 for 24 h, followed by 7 days maturation at 37 °C, 5% v/v CO_2. Afterward, cells were washed twice with warm HBSS and incubated with HBSS supplemented with HEPES (10 mM; Acros Organics, New Jersey, USA), pH 7.4 and containing fluorescein (1 μM; Sigm-Aldrich, Zwijndrecht, the Netherlands), in absence or presence of OAT1 inhibitor, probenecid (500 μM; Sigma-Aldrich, Zwijndrecht, the Netherlands) for 10 min at 37 °C, 5% v/v CO_2. Next, fluorescein was removed, cells washed quickly with ice-cold HBSS to terminate the OAT1-mediated transport of fluorescein, and lysed with 0.1 M NaOH. Fluorescence was measured using Fluoroskan Ascent FL fluorescent microplate reader at excitation wavelength of 492 nm and emission wavelength of 518 nm. The measured fluorescence values were corrected for the background (NaOH), and plotted as relative fluorescein uptake.

2.19. Data Analysis

All data are presented as mean ± standard error of the mean. Statistical analysis was performed using one-way ANOVA followed by Dunnett's multiple comparison test or, where appropriate, Tukey's multiple comparison test, and a p-value <0.05 was considered significant. Software used for statistical analysis was GraphPad Prism (version 5.03; GraphPad software, La Jolla, CA, USA). All experiments were repeated independently at least three times, unless stated differently.

3. Results and Discussion

3.1. Preparation of Nanocomposite Hydrogels

Pristine multi-walled CNTs (p-MWNT) were treated with acid to introduce carboxylic functionalities on the surface and to increase their solubility and dispersibility in water. The prepared ox-MWNT were characterized prior to being incorporated in the PE PEG2000 polymer matrix. The ox-MWNT were analyzed by several techniques, which confirm their successful functionalization (Figure S1, Supporting Information). In order to prepare homogeneous nanocomposite supramolecular hydrogels, aqueous solution of ox-MWNT was added to the acetone solution of PE PEG2000. Water containing CNTs was able to replace the acetone and induce the self-assembly of DFA nanodomains of the segmented copolymer. This resulted in hydrogel formation with CNTs included in the gel matrix. Nanocomposite gels were prepared at four different concentrations of ox-MWNT: 0.5, 1.5, 3, and 6 wt% relative to the amount of PE PEG2000. **Figure 1**a shows the components used to fabricate nanocomposite hydrogels. CNTs are embedded and physically dispersed in the hydrogel matrix, with no covalent cross-links or any other type of specific interactions between CNTs and segmented copolymer, except chain adsorption and hydrophobic interactions (Figure 1b). Dried, pressed films of PE PEG2000 copolymer and four nanocomposite materials were immersed in a large excess of water for 24 h, until swollen hydrogels were obtained. PE PEG2000 gave rise to a transparent hydrogel, while all of the nanocomposite hydrogels were completely black, due to the incorporation of CNTs. At all CNT concentrations, homogeneous black disks were observed, which confirmed good dispersion of the nanotubes within the gel matrix (Figure 1c). The FT-IR spectrum of the dried PE PEG2000 hydrogel shows the characteristic peak at 1735 cm^{-1}, corresponding to the ester

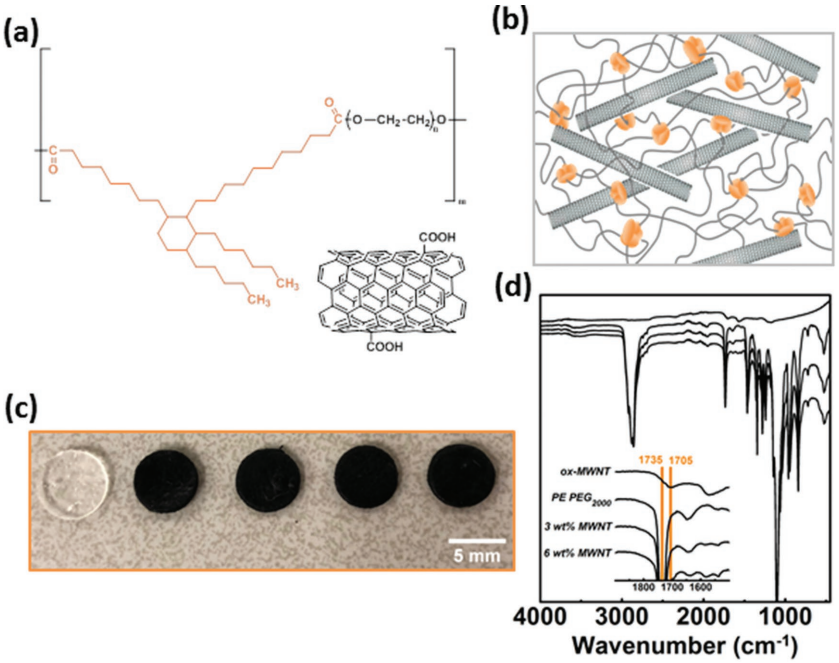

Figure 1. Fabrication and characterization of nanocomposite hydrogels. a) Structure of the components: segmented copolymer PE PEG2000 and ox-MWNT; b) schematic representation of the network of the nanocomposite gels; c) hydrogel disks, swollen in water for 24 h, from left to right: PE PEG2000 hydrogel, 0.5, 1.5, 3, and 6 wt% MWNT nanocomposites; d) ATR-FTIR spectra of ox-MWNT and hydrogels as indicated in the panel; inset displays a magnified portion of the spectra.

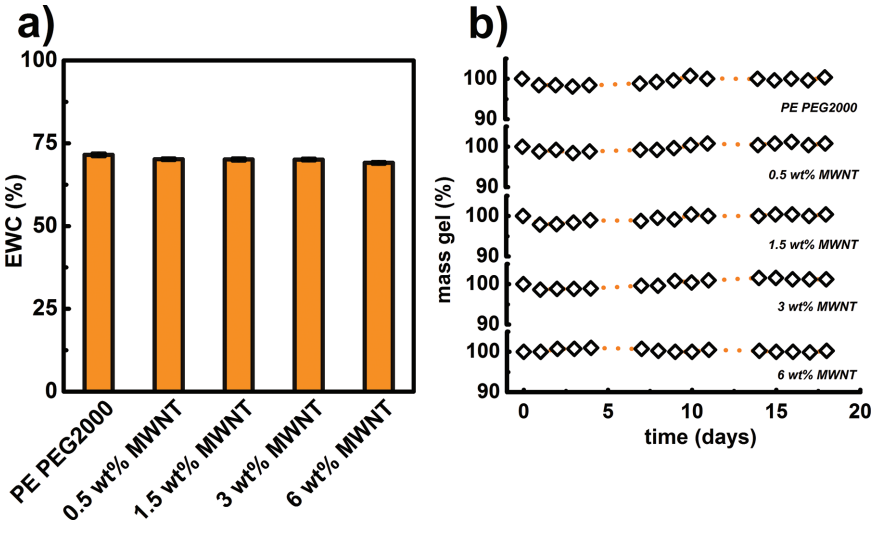

Figure 2. Swelling and stability of hydrogels. a) EWC determined for PE PEG2000 and at different MWNT amounts; b) stability of hydrogels in PBS, at 37 °C, expressed as weight variation in time. All samples are indicated in individual panels.

carbonyl stretch[25] (Figure 1d). The same vibrational stretch was observed in all of the nanocomposite hydrogels, confirming that they are based on PE PEG2000. The reference MWNT spectrum displays the stretching band at 1705 cm^{-1}, which indicates the presence of the COOH groups on their surface. However, this band was too weak to be detected in the nanocomposite gels, due to the very low concentration of MWNTs in the nanocomposites.

3.2. Equilibrium Water Content and Stability of the Nanocomposite Hydrogels

Compared to the PE PEG2000, all nanocomposite gels, regardless of the amount of the CNTs, were able to absorb the same amount of water at room temperature (RT), as determined by the gravimetric method (**Figure 2**a). EWC was determined to be between 72 wt% and 74 wt% for all samples. This suggests that dispersed nanotubes in the polymer network do not significantly alter the network structure. Therefore, the EWC is predominantly determined by the PEG to DFA ratio and by the cross-linking density. Since the bare PE PEG2000 hydrogel proved to be stable and non-eroding for 50 days at ambient conditions,[25] the stability of the nanocomposite gels was also assessed. As expected, the robust nanocomposite gels showed the same stability and solubility resistance as the parent PE PEG2000 (Figure S2, Supporting Information). This is due to the very strong hydrophobic interactions between DFA segments and consequently long relaxation time.[25] In addition, the same experiment was performed at 37 °C with samples immersed in PBS (Figure 2b). The response was the same at 37 °C as at RT for all gels, with no significant decrease in weight over a time period of 20 days. This confirmed the extraordinary stability of the present gels under physiological conditions, making them suitable for biomedical applications where high stability is desired.[33]

3.3. Internal Structure of Hydrogels

To investigate the presence of CNTs in the material structure and changes caused by their inclusion, the cross sections of all hydrogels were imaged by SEM (**Figure 3**). Freeze drying method was employed to create porous structure of the

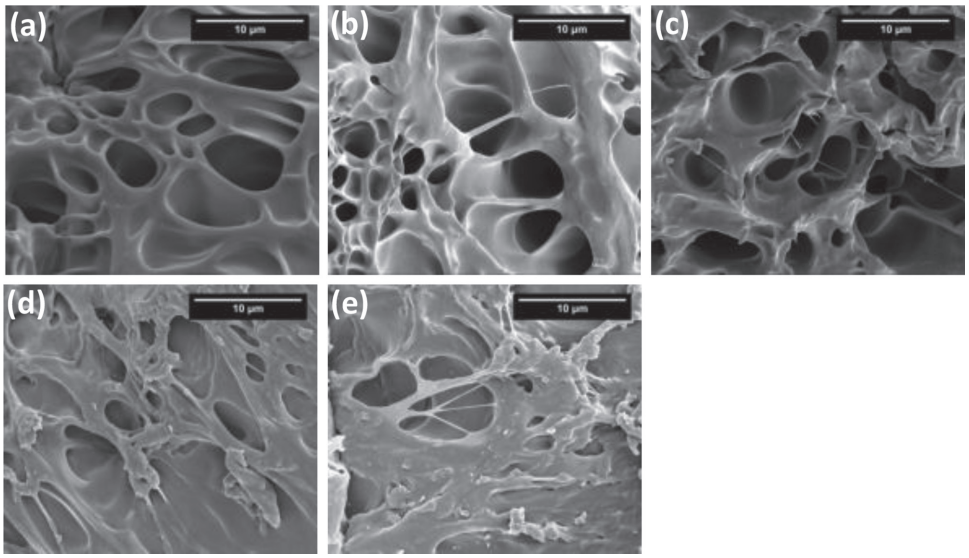

Figure 3. SEM micrographs of cross sections of a) PE PEG2000, b) 0.5, c) 1.5, d) 3, e) 6 wt% MWNT hydrogels.

samples. Clearly, the PE PEG2000 gel and nanocomposites at low MWNT content (0.5 and 1.5 wt%) appeared to be porous. However, the pore size did not seem to be related to the amount of MWNT. In addition, the nanocomposites also displayed some filamentous elements, which are typical of the MWNT morphology, confirming their presence in the network. Moreover, at higher MWNT content (3 and 6 wt%), the structure appeared to be somewhat less porous, with an overall denser and more compact architecture. Rougher pore walls were observed, due to the higher MWNT loading, along with the presence of CNT aggregates at 6 wt%. It has been reported that CNTs are able to affect the porosity of hydrogels.[15,34,35] The observed decrease of porosity could be related to the hydrophobic nature of MWNT, which allows them to interact and aggregate with DFA domains, displacing PEG components and thus reducing the network density,[15,35] although we do not exclude the possibility that the freeze drying could have caused mechanical disruption of the network structure. Overall, from SEM imaging we can conclude that MWNT were indeed successfully incorporated and dispersed in the PEG-DFA matrix.[21,35,36]

3.4. Viscoelastic Properties and Reversibility of Physical Interactions

The viscoelastic behavior of PE PEG2000 and MWNT 3 wt% nanocomposite hydrogel was studied at equilibrium swelling state and frequency sweep test was performed to evaluate the general viscoelastic behavior, both at RT and at 37 °C (**Figure 4**a,b). For both gels G′ (ω) was higher than G″ (ω) over the entire frequency range probed, which confirmed the elastic nature of hydrogels under both conditions. Surprisingly, no significant increase of stiffness of the nanocomposite, as compared to the bare hydrogel was observed. According to the theory of rubber elasticity,[37] inclusion of any type of solid particles (such as CNTs) should result in increase of stiffness, as was seen in other studies.[13,36] In this case, however, the stiffness of PE PEG2000 and 3 wt% MWNT hydrogel was quite similar (in the order of $\approx 10^5$ Pa at 25 °C). Interestingly, the opposite effect has also been reported, where upon addition of CNT to the hydrogel the stiffness was reduced.[15,38] This was attributed to the high aspect ratio of CNTs, which created a large surface for interaction with polymer chains, reducing their mobility next to CNTs and, consequently, decreasing crosslinking density.[39]

We hypothesize that in our system MWNT are embedded very efficiently in the PEG-DFA matrix. PEG-DFA hydrogel is characterized by apolar nanodomains within the hydrophilic PEG environment. Being characterized by COOH hydrophilic groups and by the apolar surface due to extensive C=C structure, we suggest that MWNT are able to interact with DFA aggregates, while still being efficiently dispersed within the PEG matrix. Therefore, they most likely do not affect cross-link density, which is why the nanocomposite hydrogel exhibited the same stiffness as the control. A similar conclusion was drawn from EWC measurements, which showed that EWC did not change upon addition of MWNT, suggesting that they do not disturb the network structure and cross-link density. This observation might be related to the purely physical nature of the interactions in this nanocomposite system, whereas most reported studies on CNT-based nanocomposites are covalently cross-linked. We do not consider the lack of stiffening by the MWNT as a drawback, because a stiffness of $\approx 10^5$ Pa of the nanocomposite is sufficient for many applications.[40]

Subsequently, the ability of the nanocomposite hydrogel to recover its original stiffness after cessation of shear was tested. Recoverability is a very important feature if the gel is to be processable. To test this, large amplitude strain response of the MWNT 3 wt% and PE PEG2000 hydrogels was performed (Figure 4c,d). First, G′ (ω) and G″ (ω) were monitored at a constant strain $\gamma = 0.1\%$ and at a frequency $\omega = 1$ rad s^{-1} for 200 s. G′ (ω) was higher than G″ (ω) for both gels, confirming that the gels were solid-like. Next, the strain was increased to $\gamma = 200\%$ and kept constant, while frequency remained unchanged for 200 s. In this phase, the network structure was broken, G″ (ω) was higher than G′(ω) and the samples were in a liquid-like, viscous state. In the next step, the strain was reduced back to 0.1% to assess recovery of the stiffness. For the PE PEG2000

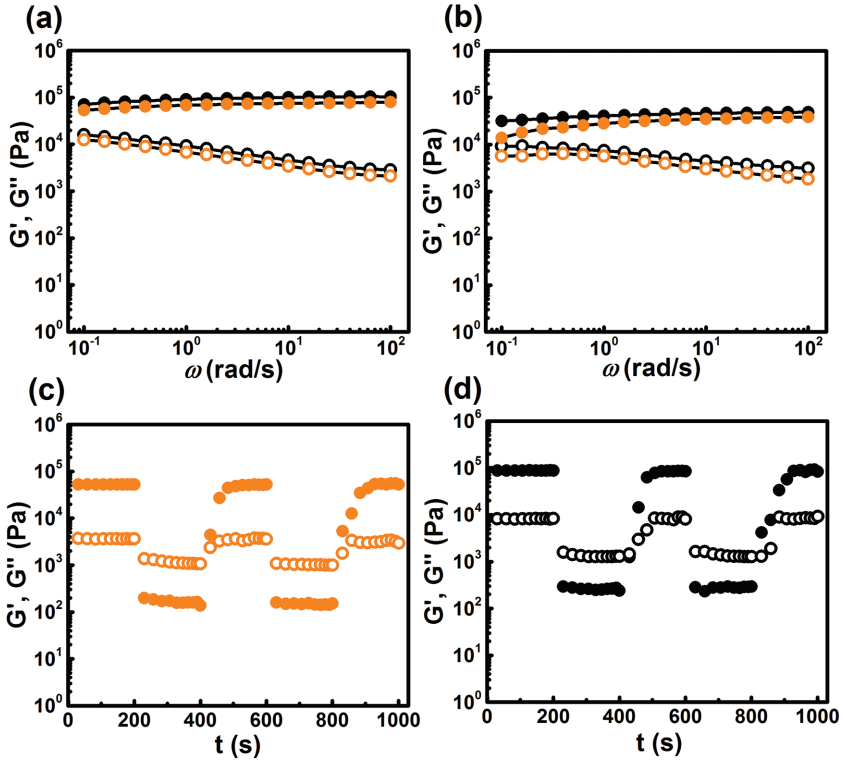

Figure 4. Frequency sweep of PE PEG2000 and 3 wt% MWNT nanocomposite at $\omega = 1$ rad s^{-1} and $\gamma = 0.1\%$, at a) 25 °C and b) 37 °C; large amplitude strain test for c) PE PEG2000 and d) 3 wt% MWNT nanocomposite. Orange symbols, PE PEG2000; black symbols, 3 wt% MWNT nanocomposite; closed symbols, G′; open symbols, G″.

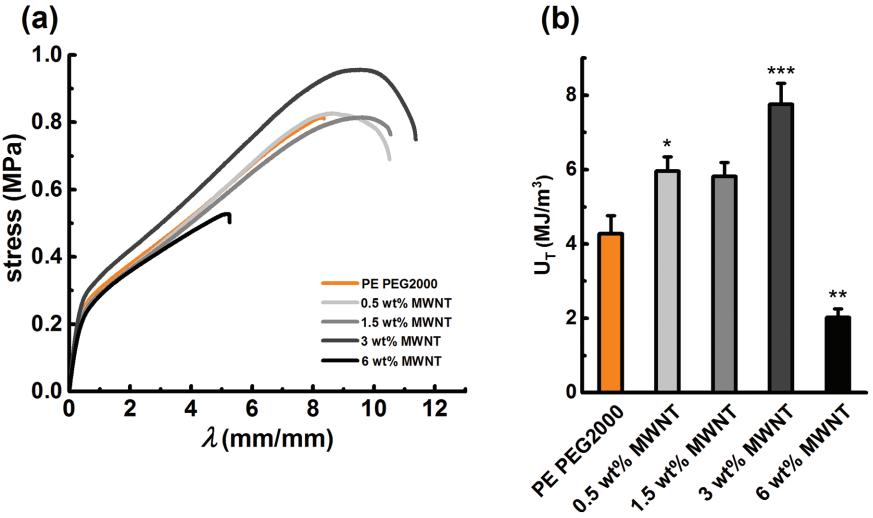

Figure 5. Tensile properties of nanocomposites. a) Stress versus displacement of PE PEG2000 and nanocomposite hydrogels at different MWNT contents, as indicated in the panel; b) comparison of tensile toughness of PE PEG2000 as a function of MWNT concentration. $*p < 0.05$, $**p < 0.01$, $***p < 0.001$ as compared to the PE PEG2000 (one-way ANOVA, Dunnett's multiple comparison test).

sample, full recovery took ≈100 s, whereas the MWNT 3 wt% nanocomposite recovered after ≈125 s. This behavior was reproducible for the second consecutive deformation cycle for both samples. Based on these findings, we conclude that the presence of MWNTs did not interfere with the process of reformation of hydrophobic associations between DFA when the strain was removed. Therefore, nanocomposites prepared in this way are fully reversible and can be processed like PE PEG2000,[25] which widens their potential applications.

3.5. Mechanical Properties and Toughness

To assess the effect that CNTs exert on the mechanical properties and toughness of the hydrogels, uniaxial tensile testing was performed on both PE PEG2000 and MWNT containing hydrogels, at equilibrium swelling and at a strain rate of 10 mm min^{-1}. The results are plotted as stress versus displacement (**Figure 5**a). The values of the determined parameters tensile modulus E_T, tensile strength σ_T, displacement λ, and tensile toughness U_T for all samples are listed in **Table** 1.

The tensile modulus for 0.5 wt% MWNT and 1.5 wt% MWNT samples barely showed any improvement compared to the PE PEG2000. The same was observed for the tensile strength. However, a significant increase for both E_T and σ_T was found for 3 wt% MWNT nanocomposite, as compared to the PE PEG2000, with E_T increasing from 0.73 to 0.88 MPa and σ_T increasing from 0.80 MPa for PE PEG2000 to 0.96 MPa for 3 wt% MWNT, respectively. This effect is most likely due to favorable physical interactions between MWNT and polymer chains, creating additional entanglements at 3 wt%. Furthermore, elongation at break (expressed as displacement λ) increased as a function of MWNT content, with elongation at break increasing from 8.27 for PE PEG2000 to 11.37 at 3 wt% MWNT content corresponding to an increase of 37%. Other mechanical parameters E_T, σ_T, and U_T showed a similar trend, with toughness increasing from 4.28 MJ m^{-3} for PE PEG2000 (in accordance with previous results[25]) to 7.76 MJ m^{-3} in the 3 wt% MWNT hydrogel, an increase of more than 80% (Figure 5b and Table 1).

However, when the concentration of MWNT was increased further to 6 wt%, a significant deterioration of all of the tensile parameters was observed. The toughness was reduced to 2 MJ m^{-3}, less than half of the value for the parent PE PEG2000 gel. Similar CNT-dependent trends were reported for other nanocomposite materials.[23] We suggest that at higher CNT concentrations, CNTs were less well dispersed in the matrix[24] and formed bundled aggregates which might have even compromised self-assembly of DFA nanodomains, resulting in a less uniform network. SEM images (Figure 3e) of 6 wt% nanocomposite hydrogel indeed show the presence of CNT aggregates. Rather than reinforcing the gel, these aggregates acted as defects, which led to stress concentration and material failure at lower strain. Most likely, the combined effects of hydrogel porosity, amount of CNTs, uniformity of their dispersion and their physical interaction with PE PEG2000 are responsible for the observed trends in tensile performance.[23]

In conclusion, improvement of mechanical performance by increasing CNT content, as reported in other works on nanocomposites,[12,41,42] is confirmed in the present CNT-based nanocomposite hydrogels, but the effect is lost at a CNT content of more than 3%.

Table 1. Tensile properties of PE PEG2000 and nanocomposite hydrogels

Sample	E_T [MPa]	σ_T [MPa]	λ [mm/mm]	U_T [MJ m^{-3}]
PE PEG2000	0.73 ± 0.03	0.80 ± 0.06	8.27 ± 0.29	4.28 ± 0.48
0.5 wt% MWNT	0.75 ± 0.03	0.81 ± 0.03	10.40 ± 0.34	5.96 ± 0.39
1.5 wt% MWNT	0.72 ± 0.07	0.80 ± 0.02	10.29 ± 0.34	5.82 ± 0.37
3 wt% MWNT	0.88 ± 0.02	0.96 ± 0.01	11.37 ± 0.81	7.76 ± 0.56
6 wt% MWNT	0.72 ± 0.04	0.51 ± 0.03	5.35 ± 0.52	2.02 ± 0.23

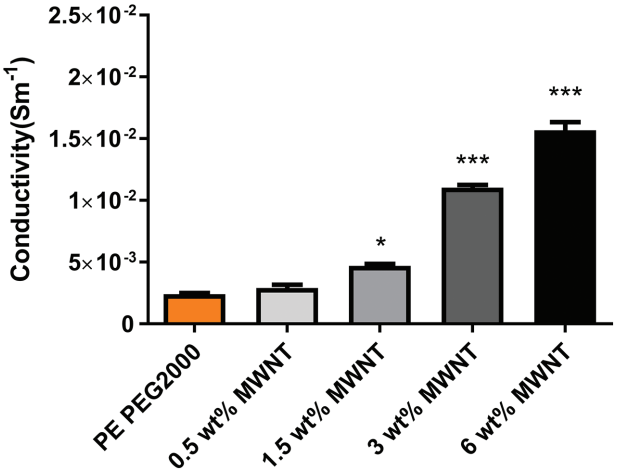

Figure 6. Electrical conductivity of PE PEG2000 and nanocomposite hydrogels at different MWNT concentrations. $*p < 0.05$, $***p < 0.001$ as compared to the PE PEG2000 (one-way ANOVA, Dunnett's multiple comparison test).

3.6. Electrical Conductivity of the Nanocomposites

It is known that CNT-based materials are able to conduct electricity,[14,15,43] due to the formation of conductive pathways of dispersed CNTs.[15,16] Therefore, resistivity measurements were performed on the present hydrogels, and the conductivity was calculated (**Figure 6**). As expected, the nanocomposites showed an increasing trend in conductivity in MWNT concentration-dependent manner. The hydrogel without MWNT had a conductivity of 2.4–10^{-3} S m^{-1}, the value due to eventual impurities and CO_2 dissolved in water from air,[14,44] and increased to 4.7–10^{-3} S m^{-1} upon inclusion of 1.5 wt% of MWNT. At 3 and 6 wt% MWNT content, the conductivities were $1.1 \cdot 10^{-2}$ S m^{-1} and $1.6 \cdot 10^{-2}$ S m^{-1}, corresponding to a total increase by 358% and 566%, respectively. The observed conductivity values were in line with other work, where similar conductivity was shown to be relevant for supporting growth and improving nerve cell response.[14] This property might be useful for a variety of applications, such as biosensors and electrically conductive scaffolds.[14,45–47]

3.7. Cytocompatibility of the PE PEG2000 and MWNT Nanocomposite Hydrogels

In order to determine cytocompatibility of the nanocomposites, ciPTEC and HeLa cells were employed. HeLa cells were used as suggested by ISO 10993-5[29,48] because of their wide use in biocompatibility studies. In addition, we opted for kidney epithelial cells as an example of less robust cell line compared to HeLa, given their susceptibility to many toxic agents and substances, including drugs such as cisplatin.[49] Also, ciPTEC represent a good choice considering that CNTs are in part excreted by kidneys.[50] Moreover, it has been shown that human proximal tubule epithelial cells were able to adhere and grow on substrates characterized by high stiffness,[51] such as the present hydrogels.

To evaluate hydrogels effect on ciPTEC viability, the gel extract test was performed. According to ISO 10993-5,[29] gels were incubated at 37 °C, CO_2 5% in complete culture medium (containing 10% FCS) for either 1 or 7 days, allowing for eventual elution of hydrogel components in the medium. Prior to the viability assay, ciPTEC were allowed to mature at 37 °C for 7 days as reported previously.[27,28] Upon maturation, the cells were exposed to complete cell culture media containing eventual gel leachables. Latex was used as negative control. Cell viability was hardly affected by hydrogel components derived from a 1 day elution test, regardless of the incubation time (24 or 48 h), with values remaining well above 90% (**Figure 7**a). However, when ciPTEC cells were exposed to medium derived from 7 days elution test, cell viability was slightly reduced, especially after 48 h of exposure (Figure 7b). Here, a MWNT dose-dependent trend was observed, with nanocomposites at 3 wt% and 6 wt% of MWNT reducing cell viability by nearly 20% and 25%, respectively. The same viability tests were repeated with HeLa cells (Figure S3, Supporting Information). HeLa cells did not present any alterations in viability, regardless of the hydrogel composition, elution time, or exposure time. The reduction of ciPTEC-OAT1's viability, but not that of HeLa cells, at higher MWNT loading most likely indicates that there might have been a release of rather small amount of CNTs, which effect on cell viability is cell type specific.

In addition to the elution test indicated by ISO 10993-5 for cytotoxicity, the viability assay upon direct contact of cells with hydrogel pieces (1 mm diameter, 0.85 mm thickness) was performed. The co-incubation of cells with hydrogels was done for 24 h and 48 h, showing that HeLa cell viability was maintained at high levels compared to the untreated controls (Figure S4, Supporting Information). However, it should be noted that in this test hydrogel disks might have had exerted external pressure on cell monolayers, thus slightly affecting cell viability.[52]

Furthermore, to observe cell viability when grown on top of the hydrogels, a live/dead assay was carried out. Prior to cell seeding, all hydrogels were coated with L-DOPA to allow ciPTEC cell adhesion on the surface, as previously reported for other types of biomaterials.[30,31,53] After 7 days of maturation, cells were stained with calcein-AM and ethidium homodimer-1 to distinguish live (green) from dead (red) cells. Obtained images show that none of the gels caused any significant cell death, as the majority of cells were stained green, confirming cytocompatibility of all examined hydrogels (Figure S5, Supporting Information).

Additionally, the ability of cells to proliferate when grown on hydrogels was assessed. Gels were first coated with L-DOPA, as discussed previously and cells were seeded at a low density. Cell metabolic activity, reflecting the number of cells, was evaluated at designated time periods. Figure 7c shows increased fluorescent signal and, therefore, increased metabolic activity over time, indicating the ability of cells to proliferate on hydrogel surface, regardless of the material composition. After 1 day of culture there was higher activity observed on CNT-based hydrogels, compared to the pure PE PEG2000. Following 4 days of culture, higher number of cells was observed on all hydrogels, with the highest values for PE PEG2000 and 0.5 wt% MWNT. Anyway, after culturing for 7 days all numbers were nearly similar, suggesting a comparable cell proliferation rate on all

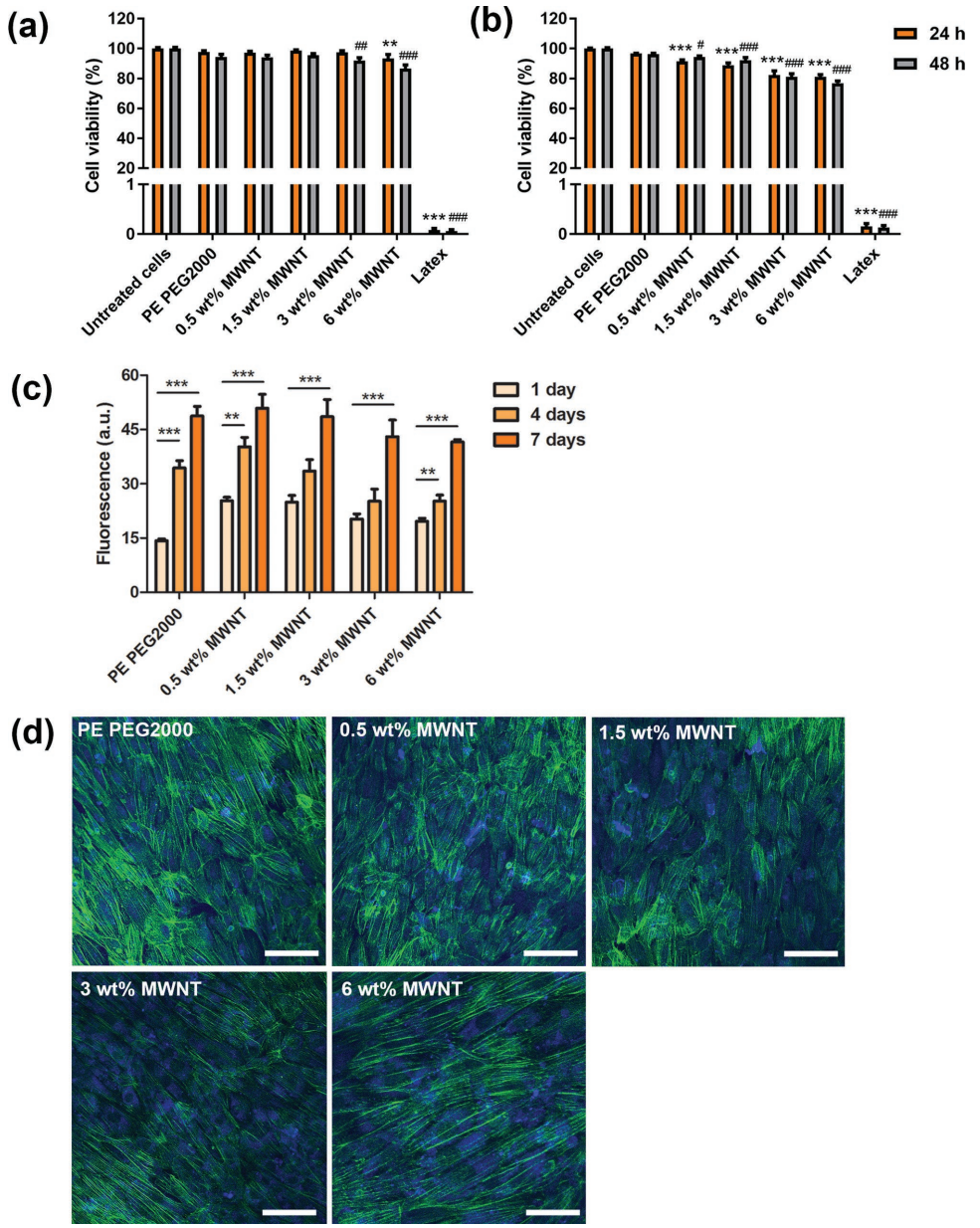

Figure 7. Cytocompatibility of the nanocomposite hydrogels at different MWNT concentrations and cell proliferation. ciPTEC-OAT1 viability after 24 and 48 h exposure to the culture medium containing hydrogel extracts following a) 1 day and b) 7 days elution test; latex is used as a negative control; $^{**}p < 0.01$, $^{***}p < 0.001$, as compared to the corresponding 24 h untreated controls; $\#p < 0.05$, $\#\#p < 0.01$, $\#\#\#p < 0.001$, as compared to the corresponding 48 h untreated controls (one-way ANOVA, Tukey's multiple comparison test). c) ciPTEC-OAT1 proliferation on L-DOPA coated hydrogels, after 1, 4, and 7 days; d) representative images (25× magnification) of ciPTEC-OAT1 cultured on L-DOPA coated hydrogels for 7 days; Actin filaments (green) and DAPI nuclear staining (blue); scale bar 10 µm; $^{**}p < 0.01$, $^{***}p < 0.001$, compared to the corresponding gel sample with the cell proliferation of 1 day (one-way ANOVA, Dunnett's multiple comparison test).

hydrogels. These results support the findings regarding nanocomposites cytocompatibility.

Moreover, cells grown on top of the hydrogels were visualized, showing that all hydrogels were able to support cell growth, adhesion, and spreading, leading to a complete surface coverage (Figure 7d).

Finally, in order to show that ciPTEC maintain their normal function when grown on hydrogels, OAT-1 activity was assessed. As described, OAT-1 is located at the basolateral membrane of PTEC and is responsible for the uptake of many drugs, xenobiotics, and uremic waste molecules from the blood compartment.[27,28,54] Its activity can easily be measured using a fluorescent substrate, such as fluorescein, via determination of its intracellular accumulation.[53] This measurement in the presence or absence of the OAT-1 inhibitor—probenecid, directly relates to the OAT-1 uptake activity. Cells grown on all gels retained their OAT-1 activity, which was supported by the reduction of fluorescein uptake in the presence

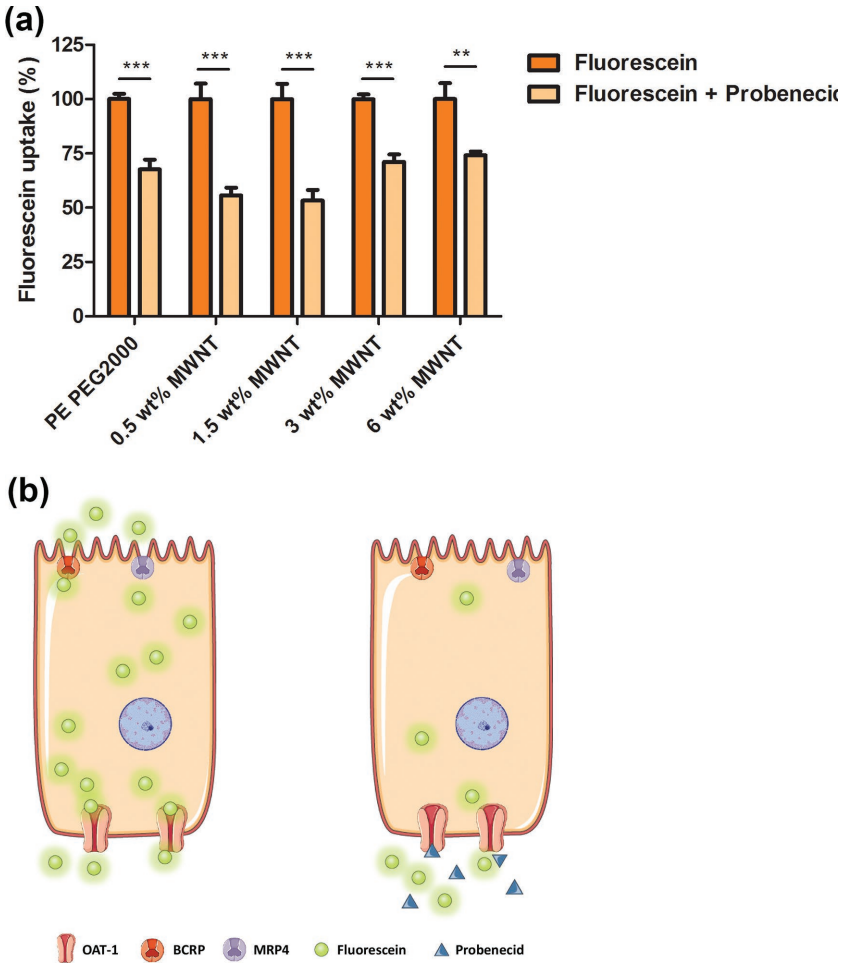

Figure 8. Cell function on the nanocomposite hydrogels at different MWNT concentrations. a) OAT1 activity determined by 10 min fluorescein (1 μM) uptake in the absence or presence of probenecid (500 μM); b) schematic representation of ciPTEC-OAT1 transport activity; $^{**}p < 0.01$, $^{***}p < 0.001$ (one-way ANOVA, Tukey's multiple comparison test).

of probenecid as compared to the uptake in normal conditions (**Figure 8**).

Observed results of cytocompatibility are in line with previous literature, showing good compatibility of CNT-based hydrogels with different cell types, such as neurons, cardiomyocytes, and human mesenchymal stem cells (hMSC).[14,55,56] Here, we show that our novel nanocomposite hydrogels are also cytocompatible, support cell growth and proliferation, and do not compromise cell activity and function, which are highly desired features when hydrogels are intended for biomedical applications.

4. Conclusions

Physical nanocomposite hydrogels based on CNTs were successfully fabricated. MWNTs were homogeneously incorporated in the matrix of supramolecular PEG-DFA hydrogel and the resulting nanocomposites were fully characterized. Hydrogels presented fully reversible shear thinning, demonstrating flow processability even in the presence of MWNT, which is an advantageous feature in combination with an easy and scalable preparation procedure.

Furthermore, it was shown that hydrogels presented increasing electrical conductivity, due to the presence of CNTs. A remarkable increase of 80% in toughness was achieved by incorporating 3 wt% of MWNT.

Overall, the hydrogels displayed some highly desirable features, including tunable mechanical and electrical properties, while maintaining other features characteristic of the parent PEG-DFA supramolecular hydrogel, such as recoverability. These nanocomposites also exhibited remarkable biocompatibility, regardless of the CNT content, suggesting their safe use for biomedical applications. We speculate that due to very favourable interactions with cells, good cytocompatibility and electrical conductivity, these gels could be used in the future as supporting scaffolds for different cell types, in particular electrically active cells, such as cardiomyocytes and neurons.

Supporting Information

Supporting Information is available from the Wiley Online Library or from the author.

Acknowledgements

Marko Mihajlovic would like to thank Dr. René Lafleur for helping with acquisition of TEM images and Ingeborg Schreur-Piet for assistance with SEM imaging. Milos Mihajlovic would like to thank Dr. Silvia Mihaila for helpful discussions. This research was funded by the Marie Curie ITN project SASSYPOL (grant no. 607602, EU-FP7-PEOPLE-2013-ITN) and by the Ministry of Education, Culture, and Science of the Netherlands (Gravity program 024.001.035). Also, Milos Mihajlovic and Rosalinde Masereeuw would like to acknowledge financial support of the Marie Curie ITN project BIOART (grant no. 316690, EU-FP7-PEOPLE-2012-ITN).

Conflict of Interest

The authors declare no conflict of interest.

Keywords

biocompatibility, electrical conductivity, multi-walled carbon nanotubes, nanocomposite supramolecular hydrogel, tensile toughness

Received: May 8, 2018
Revised: July 9, 2018
Published online: August 7, 2018

[1] N. Annabi, A. Tamayol, J. A. Uquillas, M. Akbari, L. E. Bertassoni, C. Cha, G. Camci-Unal, M. R. Dokmeci, N. A. Peppas, A. Khademhosseini, *Adv. Mater.* **2014**, *26*, 85.
[2] S. Van Vlierberghe, P. Dubruel, E. Schacht, *Biomacromolecules* **2011**, *12*, 1387.
[3] J. L. Drury, D. J. Mooney, *Biomaterials* **2003**, *24*, 4337.
[4] A. S. Hoffman, *Adv. Drug Deliv. Rev.* **2002**, *54*, 3.
[5] N. A. Peppas, J. Z. Hilt, A. Khademhosseini, R. Langer, *Adv. Mater.* **2006**, *18*, 1345.
[6] K. Haraguchi, *Curr. Opin. Solid State Mat. Sci.* **2007**, *11*, 47.
[7] F. Song, X. Li, Q. Wang, L. Liao, C. Zhang, *J. Biomed. Nanotechnol.* **2015**, *11*, 40.
[8] D. Janas, S. Boncel, K. K. K. Koziol, *Carbon* **2014**, *73*, 259.
[9] K. K. R. Datta, A. Achari, M. Eswaramoorthy, *J. Mater. Chem. A* **2013**, *1*, 6707.
[10] L. Wei, N. Hu, Y. Zhang, *Materials* **2010**, *3*, 4066.
[11] K. Z. Gao, Z. Q. Shao, X. Wang, Y. H. Zhang, W. J. Wang, F. J. Wang, *RSC Adv.* **2013**, *3*, 15058.
[12] L. Q. Liu, A. H. Barber, S. Nuriel, H. D. Wagner, *Adv. Funct. Mater.* **2005**, *15*, 975.
[13] H. U. Rehman, Y. J. Chen, Y. L. Guo, Q. Du, J. Zhou, Y. P. Guo, H. N. Duan, H. Li, H. Z. Liu, *Composites, Part A* **2016**, *90*, 250.
[14] X. F. Liu, A. L. Miller, S. Park, B. E. Waletzki, A. Terzic, M. J. Yaszemski, L. C. Lu, *J. Mat. Chem. B* **2016**, *4*, 6930.
[15] K. Shah, D. Vasileva, A. Karadaghy, S. P. Zustiak, *J. Mat. Chem. B* **2015**, *3*, 7950.
[16] R. A. MacDonald, C. M. Voge, M. Kariolis, J. P. Stegemann, *Acta Biomater.* **2008**, *4*, 1583.
[17] B. L. Guo, P. X. Ma, *Biomacromolecules* **2018**, *19*, 1764.
[18] M. C. Serrano, M. C. Gutierrez, F. del Monte, *Prog. Polym. Sci.* **2014**, *39*, 1448.
[19] C. M. Homenick, H. Sheardown, A. Adronov, *J. Mater. Chem.* **2010**, *20*, 2887.
[20] M. K. Bayazit, L. S. Clarke, K. S. Coleman, N. Clarke, *J. Am. Chem. Soc.* **2010**, *132*, 15814.
[21] W. F. Dong, C. G. Huang, Y. Wang, Y. J. Sun, P. M. Ma, M. Q. Chen, *Int. J. Mol. Sci.* **2013**, *14*, 22380.
[22] V. Saez-Martinez, A. Garcia-Gallastegui, C. Vera, B. Olalde, I. Madarieta, I. Obieta, N. Garagorri, *J. Appl. Polym. Sci.* **2011**, *120*, 124.
[23] Y. Y. Huang, Y. D. Zheng, W. H. Song, Y. X. Ma, J. Wu, L. Z. Fan, *Composites, Part A* **2011**, *42*, 1398.
[24] B. Joddar, E. Garcia, A. Casas, C. M. Stewart, *Sci. Rep.* **2016**, *6*, 12.
[25] M. Mihajlovic, M. Staropoli, M. S. Appavou, H. M. Wyss, W. Pyckhout-Hintzen, R. P. Sijbesma, *Macromolecules* **2017**, *50*, 3333.
[26] A. Pistone, A. Ferlazzo, M. Lanza, C. Milone, D. Iannazzo, A. Piperno, E. Piperopoulos, S. Galvagno, *J. Nanosci. Nanotechnol.* **2012**, *12*, 5054.
[27] T. T. G. Nieskens, J. G. P. Peters, M. J. Schreurs, N. Smits, R. Woestenenk, K. Jansen, T. K. van der Made, M. Roring, C. Hilgendorf, M. J. Wilmer, R. Masereeuw, *Aaps J.* **2016**, *18*, 465.
[28] M. J. Wilmer, M. A. Saleem, R. Masereeuw, L. Ni, T. J. van der Velden, F. G. Russel, P. W. Mathieson, L. A. Monnens, L. P. van den Heuvel, E. N. Levtchenko, *Cell Tissue Res.* **2010**, *339*, 449.
[29] ISO 10993-5:2009, Biological evaluation of medical devices—Part 5: Tests for in vitro cytotoxicity, 3rd ed., **2009**.
[30] C. M. S. Schophuizen, I. E. De Napoli, J. Jansen, S. Teixeira, M. J. Wilmer, J. G. J. Hoenderop, L. P. W. Van den Heuvel, R. Masereeuw, D. Stamatialis, *Acta Biomater.* **2015**, *14*, 22.
[31] F. Hulshof, C. Schophuizen, M. Mihajlovic, C. van Blitterswijk, R. Masereeuw, J. de Boer, D. Stamatialis, *J. Tissue Eng. Regen. Med.* **2018**, *12*, E817.
[32] M. Ni, J. C. M. Teo, M. S. bin Ibrahim, K. Y. Zhang, F. Tasnim, P. Y. Chow, D. Zink, J. Y. Ying, *Biomaterials* **2011**, *32*, 1465.
[33] K. L. Spiller, S. A. Maher, A. M. Lowman, *Tissue Eng. Part B-Rev.* **2011**, *17*, 281.
[34] S. R. Shin, S. M. Jung, M. Zalabany, K. Kim, P. Zorlutuna, S. B. Kim, M. Nikkhah, M. Khabiry, M. Azize, J. Kong, K. T. Wan, T. Palacios, M. R. Dokmeci, H. Bae, X. W. Tang, A. Khademhosseini, *ACS Nano* **2013**, *7*, 2369.
[35] Y. S. Chen, P. C. Tsou, J. M. Lo, H. C. Tsai, Y. Z. Wang, G. H. Hsiue, *Biomaterials* **2013**, *34*, 7328.
[36] S. R. Shin, H. Bae, J. M. Cha, J. Y. Mun, Y. C. Chen, H. Tekin, H. Shin, S. Farshchi, M. R. Dokmeci, S. Tang, A. Khademhosseini, *ACS Nano* **2012**, *6*, 362.
[37] B. E. J. E. Mark, *Rubberlike Elasticity: A Molecular Primer*, 2nd ed., Cambridge University Press, Cambridge, NY, **2007**.
[38] S. Sathaye, A. Mbi, C. Sonmez, Y. C. Chen, D. L. Blair, J. P. Schneider, D. J. Pochan, *Wiley Interdiscip. Rev.: Nanomed. Nanobiotechnol.* **2015**, *7*, 34.
[39] T. Ramanathan, H. Liu, L. C. Brinson, *J. Polym. Sci., Part B-Polym. Phys.* **2005**, *43*, 2269.
[40] A. K. Gaharwar, N. A. Peppas, A. Khademhosseini, *Biotechnol. Bioeng.* **2014**, *111*, 441.
[41] P. C. Ma, N. A. Siddiqui, G. Marom, J. K. Kim, *Composites, Part A* **2010**, *41*, 1345.
[42] Y. Z. Bin, M. Mine, A. Koganernaru, X. W. Jiang, M. Matsuo, *Polymer* **2006**, *47*, 1308.
[43] Z. X. Deng, Y. Guo, X. Zhao, P. X. Ma, B. L. Guo, *Chem. Mat.* **2018**, *30*, 1729.
[44] R. M. Pashley, M. Rzechowicz, L. R. Pashley, M. J. Francis, *J. Phys. Chem. B* **2005**, *109*, 1231.
[45] S. Bosi, A. Fabbro, C. Cantarutti, M. Mihajlovic, L. Ballerini, M. Prato, *Carbon* **2016**, *97*, 87.
[46] G. Cirillo, S. Hampel, U. G. Spizzirri, O. I. Parisi, N. Picci, F. Iemma, *Biomed. Res. Int.* **2014**, 17.
[47] V. Martinelli, G. Cellot, F. M. Toma, C. S. Long, J. H. Caldwell, L. Zentilin, M. Giacca, A. Turco, M. Prato, L. Ballerini, L. Mestroni, *ACS Nano* **2013**, *7*, 5746.
[48] W. J. Li, J. Zhou, Y. Y. Xu, *Biomed. Rep.* **2015**, *3*, 617.
[49] M. H. Hanigan, P. Devarajan, *Cancer Ther.* **2003**, *1*, 47.
[50] A. Ruggiero, C. H. Villa, E. Bander, D. A. Rey, M. Bergkvist, C. A. Batt, K. Manova-Todorova, W. M. Deen, D. A. Scheinberg, M. R. McDevitt, *Proc. Natl. Acad.Sci. U. S. A.* **2010**, *107*, 12369.
[51] J. A. Beamish, E. Chen, A. J. Putnam, *PLoS One* **2017**, *12*, e0181085.
[52] L. Jing, H. Li, R. Y. Tay, B. Sun, S. H. Tsang, O. Cometto, J. Lin, E. H. T. Teo, A. I. Y. Tok, *ACS Nano* **2017**, *11*, 3742.
[53] J. Jansen, M. Fedecostante, M. J. Wilmer, J. G. Peters, U. M. Kreuser, P. H. van den Broek, R. A. Mensink, T. J. Boltje, D. Stamatialis, J. F. Wetzels, L. P. van den Heuvel, J. G. Hoenderop, R. Masereeuw, *Sci. Rep.* **2016**, *6*, 12.
[54] F. G. Russel, R. Masereeuw, R. A. van Aubel, *Annu. Rev. Physiol.* **2002**, *64*, 563.
[55] A. K. Gaharwar, A. Patel, A. Dolatshahi-Pirouz, H. B. Zhang, K. Rangarajan, G. Iviglia, S. R. Shin, M. A. Hussain, A. Khademhosseini, *Biomater. Sci.* **2015**, *3*, 46.
[56] S. Pok, F. Vitale, S. L. Eichmann, O. M. Benavides, M. Pasquali, J. G. Jacot, *ACS Nano* **2014**, *8*, 9822.